Donor Ion-Implantation Doping into SiC

MULPURI V. RAO,[1] J. TUCKER,[1] O.W. HOLLAND,[2] N. PAPANICOLAOU,[3] P.H. CHI,[4] J.W. KRETCHMER,[5] and M. GHEZZO[5]

1.—Department of Electrical and Computer Engineering, George Mason University, Fairfax, VA 22030. 2.—Oak Ridge National Laboratory, Oak Ridge, TN 37831. 3.—Naval Research Laboratory, Washington, D.C. 20375. 4.—National Institute of Standards and Technology, Gaithersburg, MD 20899. 5.—General Electric Corporate Research and Development, Schenectady, NY 12301

In this paper, dopant electrical activation and dopant thermal stability results of As and Sb-implanted 6H-SiC epitaxial layers and N ion implantations into bulk semi-insulating (SI) 4H-SiC are presented. In addition, empirical formulas for the first four statistical moments (range, straggle, skewness, and kurtosis) of the implant depth distributions of N and P ion implants are developed in the energy range of 50 keV to 4 MeV. The nitrogen ion-implantations in SI 4H-SiC yield an acceptable (27%) room-temperature electrical activation (ratio of measured sheet carrier concentration at room-temperature to the implant dose) for N concentrations of 2×10^{19} cm^{-3}. The As and Sb implants out-diffuse during annealing and yield low (<20%) room-temperature electrical activation for implant concentrations of 10^{19} cm^{-3}. The N and P implant depth distributions in SiC can be simulated using the Pearson IV distribution function and the range statistics provided by the empirical formulas.

Key words: Activation, annealing, donors, ion-implantation, SiC

INTRODUCTION

Silicon carbide is increasingly being considered for high power,[1–3] high temperature,[4] and high frequency[5,6] device applications. Ion-implantation is the only planar, selective-area doping technique available for fabricating SiC devices. The only alternative doping method in SiC is *in-situ* doping during epitaxial growth followed by reactive ion etching to define the doped regions. Problems with this technology include a loss of planarity, which results in a low yield of integrated circuit manufacturing, and the complexity of obtaining different doping profiles for different devices on the same chip. Ion-implantation doping can solve these problems. Despite its advantages, ion-implantation in SiC has not been fully utilized in developing process technologies for device manufacturing. An accurate knowledge of range statistics of useful dopant ions in the keV to MeV energy range and the electrical activation behavior of impurities such as As and Sb have not been reported to date. One of the reasons for the slow progress of ion-implantation technology in SiC is the lack of appropriate in-house ion-implantation facilities with many SiC research groups. Most ion-implanters have limitations that restrict ion energies to less than 200 keV. Due to its high density, the range (R_p) of an ion in SiC is much less compared to that in Si. For example, a 200 keV N ion implant into Si has an R_p value of 0.44 μm, while the corresponding ion range in SiC is only 0.28 μm. Therefore, high-energy (MeV range) ion-implantation is needed to achieve the depth of doping required for high-power devices and complementary field-effect-transistors. Due to the lower ionization energies of group V donors as compared to the group III acceptor species,[7,8] the donor implants nominally give higher carrier concentrations even for moderate implant doses, whereas acceptor implants need to be performed at higher doses, which result in heavy lattice damage. This requires that acceptor implantations be performed at an elevated-temperature (ET) to suppress the formation of ion-induced damage, which is not mandatory for donor implantation.

The donor behavior of group V elements in SiC requires that the dopants occupy substitutional sites in the SiC lattice. Nitrogen is the lightest of all donor

(Received September 24, 1998; accepted November 11, 1998)

Table I. Multiple-Energy Ion-Implantation Schedules Used in this Study

Implant Number	Implant Species	Implant Volumetric Concentration (cm^{-3})	Implant Schedule Used Energy/Dose (keV/ cm^{-2})
1	As	1×10^{19}	$220/5.0 \times 10^{13}$ $140/2.5 \times 10^{13}$ $80/2.0 \times 10^{13}$ $40/1.1 \times 10^{13}$ $20/1.0 \times 10^{13}$ Total Dose: 1.16×10^{14} cm^{-2}
2	Sb	1×10^{19}	$200/2.0 \times 10^{13}$ $140/1.9 \times 10^{13}$ $80/1.4 \times 10^{13}$ $40/9.0 \times 10^{12}$ $20/8.0 \times 10^{12}$ Total Dose: 7.0×10^{13} cm^{-2}
3	N	2×10^{19}	$1100/4.0 \times 10^{14}$ $800/3.8 \times 10^{14}$ $550/3.6 \times 10^{14}$ $360/3.0 \times 10^{14}$ $240/2.6 \times 10^{14}$ $150/2.2 \times 10^{14}$ $90/1.8 \times 10^{14}$ $45/1.2 \times 10^{14}$ $20/6.6 \times 10^{13}$ Total Dose: 2.3×10^{15} cm^{-2}

species in SiC and resides predominantly on C lattice sites.[9] The relatively light weight of N (atomic mass = 14) makes it attractive for ion-implantation doping due to versatility of ion range and low lattice damage. After N, phosphorus is the lightest of the remaining group V elements and is extensively used as a donor impurity in Si technology. The P resides predominantly on Si lattice sites in SiC.[10] Previous work on N[11–18] and P[12,19–21] ion implantations in p-type 6H-SiC epitaxial layers indicated good electrical activation, thermal stability and lattice quality behavior. Electrical activation and thermal stability behavior of the other group V impurities As and Sb has not been reported to date.

In this paper, we report new dopant electrical activation and dopant thermal stability results on 6H-SiC epitaxial layers implanted with As and Sb and bulk semi-insulating (SI) 4H-SiC implanted with N. We also report empirical formulas for the first four statistical moments of the implant depth distribution, namely range, straggle, skewness, and kurtosis for N and P ion implants in the energy range 50 keV–4 MeV. These were developed by using secondary ion mass spectrometry (SIMS) experimental results published by us earlier.[11,20] Validity of these empirical formulas is checked by fitting the experimental SIMS profiles using the Pearson IV distribution function and the range statistics obtained from the empirical formulas. It has been observed that the skewness and kurtosis are necessary for accurate modeling of the implant distribution.[11] Skewness (γ) represents the tilt of the implant distribution (either toward or away from the surface), and kurtosis (β) represents the sharpness of the peak of the implant profiles compared to a standard Gaussian distribution. The empirical formulas of the range statistics are helpful for designing the implant schedules required for device fabrication and for modeling the devices.

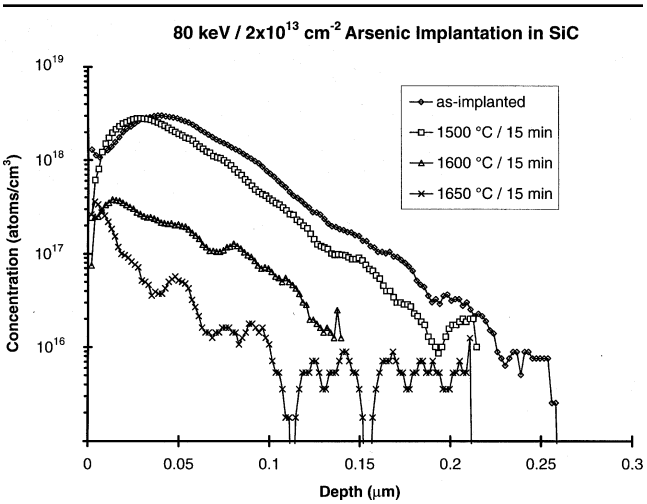

Fig. 1. SIMS depth profiles of As in elevated temperature (800°C) 80 keV/2 $\times 10^{13}$ cm^{-2} As ion-implanted 6H-SiC before and after annealing.

EXPERIMENTAL PROCEDURE

Multiple-energy As and Sb implantations were performed into 4–5 μm thick p-type epitaxial layers with 1×10^{16} cm^{-3} doping concentration grown on bulk Si face, 3.5° off-axis, <1000>, 2×10^{18} cm^{-3} carrier concentration p-type 6H-SiC substrates. We have also performed variable dose N implantations into Si face, off-axis V-doped semi-insulating bulk 4H-SiC substrates. The implants were performed using high-

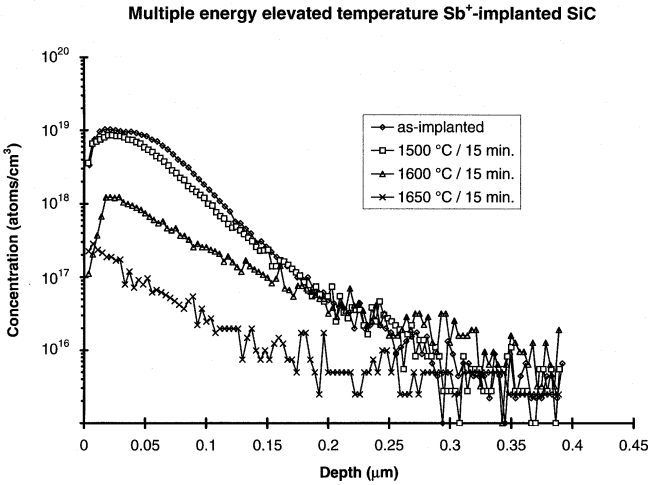

Fig. 2. SIMS depth profiles of Sb in elevated temperature (800°C) multiple-energy Sb ion-implanted 6H-SiC epilayers before and after annealing. The implant schedule used is given in Table I.

energy, high-current implanters. The implants were performed at both room-temperature and an elevated-temperature (500 or 800°C). Typical multiple-energy implantation schedules used in this study are given in Table I. Post-implantation annealing was performed in a Brew ceramic processing furnace at 1 atm. pressure in an ultra-pure Ar ambient for 15 min. The samples were enclosed in a SiC crucible to minimize deterioration of the sample surface caused by evaporation of Si at annealing temperatures greater than 1300°C. Hall-effect measurements were performed to evaluate the extent of implant activation and carrier mobility. The ohmic contacts were formed by evaporation of approximately 100 nm thick Ni with subsequent alloying at 1000–1100°C for 1–2 min in vacuum. Secondary ion mass spectrometry measurements were performed to obtain implant depth profiles before and after annealing. Details of SIMS measurements are given in Ref. 11.

RESULTS AND DISCUSSION

Arsenic and Antimony Implantations in 6H-SiC Epilayers

Both As and Sb have low diffusion coefficients in Si (about one-tenth that of P),[22] making these dopants attractive for obtaining precise doping depth profiles. The large atomic mass (74.92 for As and 121.75 for Sb) of these two species is also expected to yield shallow abrupt n-p junctions by ion-implantation. As and Sb implants in SiC were studied for these reasons. Arsenic and antimony preferentially take Si lattice sites in SiC.[23,24] Though there are few studies[24–26] on As and Sb implants in SiC, to our knowledge results of the implants' electrical activation and thermal stability have not been reported to date. The thermal stability of the As and Sb implants was studied by performing SIMS measurements on the implanted material before and after annealing at 1500, 1600, and 1650°C for 15 min. The SIMS depth profiles for the single energy As and multiple energy Sb implantation are given in Fig. 1 and Fig. 2, respectively. Unlike N and P,[12] both As and Sb severely out-diffused during annealing. The magnitude of out-diffusion increased with increasing annealing temperature. After 1650°C annealing only a small fraction (<10%) of the implanted As or Sb dopant remained in the material. The preferential evaporation of Si during high temperature annealing leaves Si vacancies at the SiC sample surface. It is well known that the stoichiometric disturbances caused by ion-implantation in compound semiconductors are in the form of lattice vacancies at the surface.[20,27,28] The concentration of vacancies at the surface increases with the atomic mass of the implant species. Since As and Sb are heavier than N and P, the concentration of Si and C vacancies at the surface is greater than the peak-implant concentration. As stated earlier, both Sb and As take Si lattice sites in SiC. The presence of a large concentration of Si vacancies at the surface coupled with low solid solubility limits[7] of As and Sb could be a driving force for the fast out-diffusion of these two dopants. Arsenic implant loss at the surface was also seen in Si substrates.[22] The high degree of out-diffusion of As and Sb is a problem when using implants of these dopants in SiC.

To study the electrical activation behavior of the As and Sb, multiple-energy implants were performed at 800°C to obtain a uniform 1×10^{19} cm^{-3} doping concentration to a depth of ~0.1 μm. The implant schedules used are given in Table I. Electrical characteristics for the As and Sb implant schedules 1 and 2 in Table I after 1500°C/15 min annealing are given in Table II. For comparison, the electrical activations measured earlier for 700°C multiple energy N and P implantations in p-type 6H-SiC epilayers are also

Table II. Electrical Characteristics of Ion-Implanted 6H-SiC Material Measured by the Hall Technique at RT

Implant Species	Implant Temperature (°C)	Total Dose, Φ (cm^{-2})	Sheet Resistance (Ω/□)	Hall Sheet Carrier Concentration n_s (cm^{-2})	Percentage Activation (n_s/Φ) × 100	Carrier Mobility (cm^2/V·s)
As	800	1.16×10^{14}	4.1×10^3	1.4×10^{13}	12	107
Sb	800	7.0×10^{13}	5.2×10^3	1.4×10^{13}	20	88
N	700	8×10^{14}	6.1×10^2	2.3×10^{14}	29	44
P	700	2.7×10^{15}	3.4×10^2	6.6×10^{14}	24	38

Note: Annealing was performed at 1500°C for 15 min.

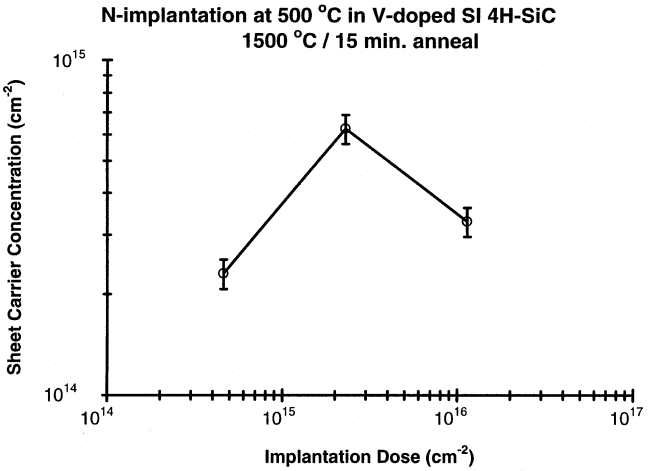

Fig. 3. Variation of sheet carrier concentration measured at room temperature with total implant dose for multiple-energy N ion implantation in V-doped bulk semi-insulating 4H-SiC. Annealing was performed at 1500°C for 15 min.

listed in Table II for the implant schedules given in Refs. 12 and 13 for P and N-implantations, respectively. For both As and Sb, the electrical activation is lower compared to that obtained for N and P implantations. This could be due to

- Deeper ionization energies of As and Sb donors compared to N and P,
- The greater amount of residual damage for these high-mass dopants which results in less electrically active, substitutional dopant in the material, or
- Low solid solubility limits of As and Sb in SiC.

Rutherford backscattering spectroscopy (RBS) measurements on ET Sb-implanted and annealed SiC indicated a scattering yield above the virgin level indicating the presence of residual damage even after 1500°C annealing which could impact activation of these impurities. For room temperature (RT), 1×10^{19} cm^{-3}, multiple-energy Sb-implanted material, the RBS yield after annealing remains close to the random level indicating a high degree of residual lattice damage. We observed a decrease in sheet carrier concentration with increasing annealing temperature due to out-diffusion of the implanted dopant at higher temperatures. The Schottky C-V depth profiling measurements on As and Sb implanted and 1500°C annealed material indicated substitutional implant concentrations of $\approx 2.5 \times 10^{18}$ cm^{-3} for both RT and 800°C implantation. Solid solubility limits for As and Sb in SiC were reported earlier in literature[7] to be much less than the substitutional implant concentration found by C-V on Schottky diodes in this study. This indicates that the low solid solubility limits of As and Sb are probably responsible for poor electrical activation of the dopant. Because of the low implant activation and thermal instability characteristics of As and Sb, we have not pursued development of empirical formulas for the range statistics of these two dopant ions.

Nitrogen Implantation in Bulk Semi-Insulating 4H-SiC

The semi-insulating SiC substrate helps to minimize parasitic device capacitances which is attractive for microwave frequency application.[5,29,30] Selective area N-implantation into semi-insulating SiC substrates facilitates inter-device isolation. At present, the epitaxial growth of V-doped SI SiC layers is not available. Hence, to make full use of SI SiC, the devices need to be fabricated within the bulk substrate. However, due to the presence of high background doping concentration and defect density in the bulk material, this technology, at first glance, does not seem very attractive. To determine if doping activations and carrier mobilities comparable to those in epitaxial layers can be achieved in bulk SI material, we have performed multiple-energy N-implantations in SI 4H-SiC to a depth of 1.0 μm. Variable dose implants were carried out to determine how the doping activation varies with the implant dose. A typical implant schedule used to obtain 2×10^{19} cm^{-3} N-concentration is given in Table I as implant No. 3. The implants were performed at 500°C. Variation of Hall sheet carrier concentration measured at RT with total N implant dose after 1500°C/15 min annealing is shown in Fig. 3. The dopant activation percentage decreased from 50% for 4×10^{18} cm^{-3} N-concentration to 3% for 1×10^{20} cm^{-3} N concentration. These values are similar to those reported for N-implants in p-type 6H- and 4H-SiC epitaxial layers.[11–18] The very low activation for 1×10^{20} cm^{-3} N-concentration is due to excessive implant lattice damage in SiC and saturation of electrically active C sites with N atoms.[15,17] The Hall carrier mobility observed for 2×10^{18} cm^{-3} carrier concentration in the lightly doped material is 90 $cm^2/V \cdot s$ which is close to the values reported in the litera-

Table III. Fitting Constants in the Empirical Formulas for Range Statistics of N and P Ion-Implantations

Ion	K_1 (μm/MeV)	K_2 (μm)	m $(MeV)^{-1}$	K_3 (μm/MeV)	K_4 (μm)	n $(MeV)^{-1}$	K_5	K_6 $(MeV)^{-1}$	K_7	p $(MeV)^{-1}$
N^+	0.472	0.601	1.85	0.0016	0.119	3.66	0.511	–0.018	0.571	3.683
P^+	0.319	0.746	0.974	0.0112	0.127	3.28	1.854	0.620	–0.196	4.040

Ion	K_8 $(MeV)^{-1}$	K_9	K_{10} (μm/MeV)	K_{11} (μm)	r $(MeV)^{-1}$	K_{12} $(cm)^{-1}$	K_{13} $(cm \cdot MeV)^{-1}$	K_{14} $(cm)^{-1}$	s $(MeV)^{-1}$
N^+	1.045	0.636	0.468	0.624	1.785	62634	138.8	50738	3.135
P^+	0.387	0.307	0.287	0.932	0.820	201237	2848.4	41583	10.36

ture for epitaxial material of similar doping concentration.[7] These results demonstrate that ion-implantation should be useful in making field-effect-transistors (FETs) and other microwave devices in bulk SI SiC.

Range Statistics of N and P Ions in 6H-SiC

Our earlier results[11–14,20] and those reported by other groups[15–18,21] suggest that both N and P ion-implantations are viable for device fabrication. In the case of N implantation, the electrical characteristics are similar irrespective of implantation temperature for implant concentrations of $\leq 4 \times 10^{19}$ cm^{-3}.[11,14] The P implants need to be performed at an elevated temperature (700–800°C) to obtain good electrical activation.[12] Because of the comparable carrier ionization energies (80±5 meV), P donors implanted at an elevated temperature give RT carrier concentrations similar to N implantations. For both N and P, for implant concentrations $\leq 4 \times 10^{19}$ cm^{-3} almost 90–100% of the implant is driven into substitutional sites during annealing and carrier concentrations close to the implant atom concentrations can be measured at 250°C due to complete ionization of the implant donor levels.[12] Because of their thermal stability during annealing and good electrical activation characteristics, the N and P implantations are attractive for device fabrication in SiC. Design of implant schedules for a specific device application requires accurate knowledge of implant range statistics at various ion energies. Computer codes like TRIM[31] cannot predict all four moments of the implant depth distributions accurately, especially at the MeV ion energy range. Because thermal diffusion technology does not exist for SiC and the range of ions in SiC is more shallow compared to Si, MeV ion-implantation is necessary for creating the deeply doped regions required for fabricating high-power devices and complementary FETs by double-implantation. For this reason, we have developed empirical formulas for the range statistics of N and P ions in 6H-SiC using our previous experimental values[11,20] obtained by analyzing the as-implanted SIMS depth profiles of single-energy N and P ion implants in the energy range 50 keV–4 MeV. Recently, we reported[20] the empirical formulas of range and straggle for P ions. In this work, we are extending this to skewness and kurtosis. In addition, fitting constants for N ions are developed in this study. The empirical formulas developed by fitting the experimental data are given below for the range (R_p), straggle (ΔR_p), skewness (γ), and kurtosis (β), implant peak concentration (N_m), and implant peak depth (R_m) of the N and P ion-implant depth distributions.

$$R_p = K_1 \cdot E - K_2 \cdot [\exp(-mE) - 1] \quad (1)$$

$$\Delta R_p = K_3 \cdot E - K_4 \cdot [\exp(-n \cdot E) - 1] \quad (2)$$

$$\gamma = K_5 \cdot \exp(-p \cdot E) - K_6 + K_7 \cdot E \quad (3)$$

$$\beta = \{[39 \cdot \gamma^2 + 48 + 6 \cdot (\gamma^2 + 4)^{3/2}]/(32 - \gamma^2)\} + K_8 \cdot E + K_9 \quad (4)$$

$$R_m = K_{10} \cdot E - K_{11} \cdot [\exp(-r \cdot E) - 1] \quad (5)$$

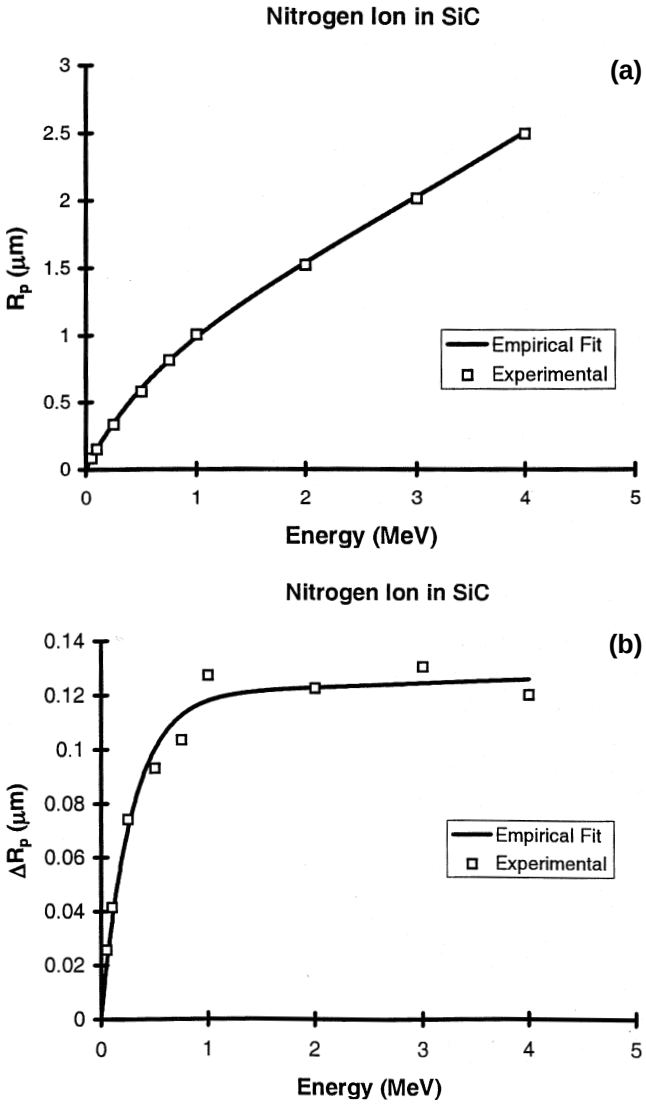

Fig. 4. Variation of (a) range, R_p and (b) straggle, ΔR_p with N ion energy in 6H-SiC. The curves are based on empirical formulas (1) and (2) with the constants given in Table III for N^+ ions.

$$N_m = \Phi \cdot [K_{12} \cdot \exp(-s\,E) - K_{13} \cdot E + K_{14}] \quad (6)$$

where E is the energy and Φ is the dose of the implant. The physical significance of the four quantities R_p, ΔR_p, γ, and β is explained in detail elsewhere.[11,20,32,33] Values for the fitting constants in Eqs. (1) to (6) for N^+ and P^+ ions are given in Table III. The experimental R_p and ΔR_p values vs N ion energy and the fitting curves for the experimental data based on Eq. (1) and Eq. (2) and constants in Table III are shown in Fig. 4 for the N^+ ions. The experimental γ and β values for various P ion energies and the fitting curves based on Eq. (3) and Eq. (4) and constants in Table III are given in Fig. 5. Using the empirical formulas (1) to (6) given above and the Pearson IV distribution,[32–34] one can construct the implant profiles for N and P ions. The experimental SIMS depth profiles for P-implants and the Pearson IV fits based on range statistics and N_m obtained from empirical formulas (1) to (6) for P ion implantations in the energy range 100 keV to 4 MeV

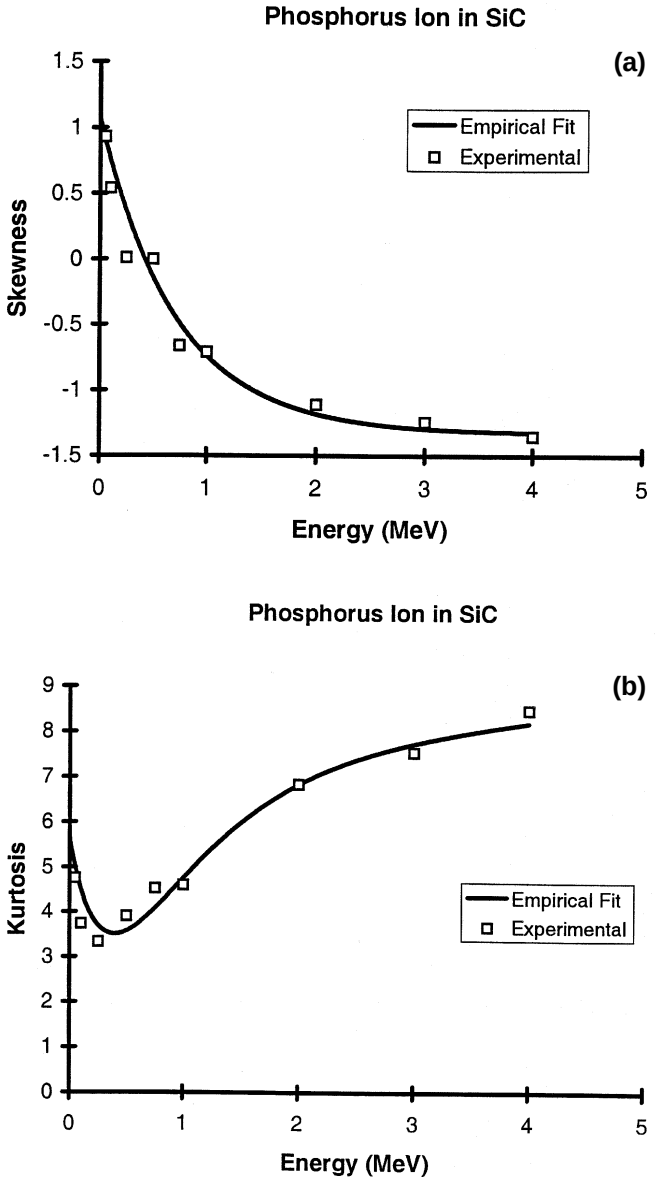

Fig. 5. Variation of (a) skewness, γ and (b) kurtosis, β with P ion energy in 6H-SiC. The curves are based on empirical formulas (3) and (4) with the constants given in Table III for P ions.

are shown in Fig. 6. Figure 6 shows the reasonable validity of the empirical formulas and Pearson IV distribution for modeling ion-implantation distributions in SiC. Note that the Pearson IV distribution gives imaginary values when β falls below $\beta_o = [39\cdot\gamma^2 + 48 + 6\cdot(\gamma^2 + 4)^{3/2}]/(32 - \gamma^2)$ since the square root of a negative number will be taken in the Pearson IV distribution formula. Therefore, the empirical formula for β [Eq. (4)] is created to avoid this problem. The fitting constants for the γ and β empirical formulas for the nitrogen ions need to be refined to obtain better Pearson IV fittings. Our experimental γ and β data for N ions scattered more than for P. The increased scattering was caused by the high background N concentration in the starting material, which interfered with the SIMS depth profiling.[11]

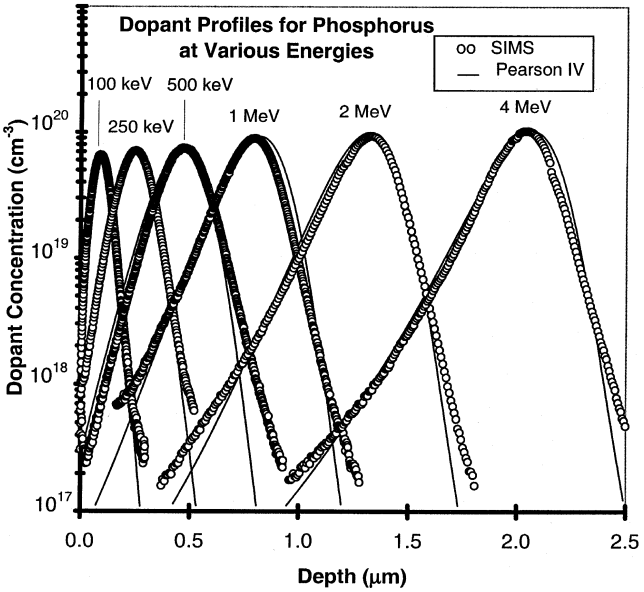

Fig. 6. Experimental SIMS depth profiles and Pearson IV depth distributions based on range statistics obtained from empirical formulas (1) to (4) for P ion implantations into 6H-SiC at various energies.

CONCLUSION

In conclusion, of the four donor dopants, N, P, As, and Sb, at present implantations of the N and P ions are effective in obtaining n-type regions in both p-type and semi-insulating SiC. Implants of these two dopants give ≥25% room temperature electrical activation (for implant concentrations $\leq 4 \times 10^{19}$ cm^{-3}) and both of these species are thermally stable during lattice damage/dopant activation annealing. The empirical formulas for the range statistics of the N and P ion implant depth distributions were developed based on the experimental results obtained by the analysis of single-energy implant SIMS depth distributions. The As and Sb implants out-diffuse during annealing and yield poor donor carrier activation even for elevated-temperature implantation, probably due to the low solid solubility limits of both dopants. More work on effective MeV energy range implant-blocking layers that can withstand high implant temperatures (≥800°C) and capping layers to protect the SiC surface during high temperature (>1400°C) annealing needs to be performed to advance ion-implantation technology in SiC. At present, an AlN capping layer appears attractive for the protection of the SiC surface during annealing for temperatures up to 1600°C.

ACKNOWLEDGMENTS

We thank Mark Ridgway of the Australian National University for his help with N ion implantations in 4H-SiC. The work at George Mason University is supported by NSF under Grant #ECS-9711128 and by DARPA-ETO (through GE) under contract #MDA972-98-C-0001. The work at Oak Ridge National Laboratory, managed by Lockheed Martin Energy Corporation for the U.S. Department of Energy, is supported by contract #DE-AC05-96 OR 22464.

REFERENCES

1. D.M. Brown, E. Downey, M. Ghezzo, J. Kretchmer, V. Krishnamurthy, W. Hennesy and G. Michon, *Solid-State Electron.* 39, 1531 (1996).
2. B.J. Baliga, *Inst. Phys. Conf. Ser.* 142, 1 (1996).
3. J.A. Cooper, Jr., M.R. Melloch, J.M. Woodall, J. Spitz, K.J. Schoen and J.P. Henning, *Mater. Sci. Forum* 264-268, 895 (1998).
4. L.V. Rozario, L.P. Sadwick, R.J. Hwu and D.B. King, *Proc. of Fourth Intl. High Temp. Electron. Conf.* (HiTec), Albuquerque, NM, June 1998, (1998), p. 29.
5. S. Sriram, G. Augustine, A.A. Burk, Jr., R.C. Glass, H.M. Hobgood, P.A. Orphanos, L.B. Rowland, T.J. Smith, C.D. Brandt, M.C. Driver and R.H. Hopkins, *IEEE Electron Device Lett.* 17*,* 369 (1996).
6. C.E. Weitzel, J.W. Palmour, C.H. Carter, Jr. and K. Nordquist, *IEEE Electron Dev. Lett.* 15, 406 (1994).
7. G.L. Harris (ed), *Properties of Silicon Carbide,*(London: INSPEC, IEE, 1995).
8. T. Stiasny and R. Helbig, *Inst. Phys. Conf. Ser. No 142*, (Bristol, U.K.: Institute of Physics, 1996), p. 389.
9. D.J. Larkin, P.G. Neudeck, J.A. Powell and L.G. Matus, *Inst. Phys. Conf. Ser.* 137, (Bristol, U.K.: Institute of Physics, 1993), p. 51.
10. N.T. Bagraev, L.E. Klyachkin and V.L. Sukhanov, *Solid State Electron.* 36, 1741 (1993).
11. J. Gardner, M.V. Rao, O.W. Holland, G. Kelner, D.S. Simmons, P.H. Chi, J.M. Andrews, J. Kretchmer and M. Ghezzo, *J. Electron. Mater.* 25, 885 (1996).
12. J. Gardner, A. Edwards, M.V. Rao, N. Papanicolaou, G. Kelner, O.W. Holland, M.A. Capano, M. Ghezzo and J. Kretchmer, *J. Appl. Phys.* 83, 5118 (1998).
13. J. Gardner, M.V. Rao, Y.L. Tian, O.W. Holland, E.G. Roth, P.H. Chi and I. Ahmad, *J. Electron. Mater.* 26, 144 (1997).
14. D. Dwight, M.V. Rao, O.W. Holland, G. Kelner, P.H. Chi, J. Kretchmer and M. Ghezzo, *J. Appl. Phys.* 82, 5327 (1997).
15. T. Kimoto, N. Inoue and H. Matsunami, *Phys. Stat. Sol. (a)* 162, 263 (1997).
16. T. Kimoto, A. Itoh, N. Inoue, O. Takemura, T. Yamamoto, T. Nakajima and H. Matsunami, *Mater. Sci. Forum* 264-268, 675 (1998).
17. N. Inoue, A. Itoh, T. Kimoto, H. Matsunami, T. Nakata and M. Inoue, *J. Electron. Mater.* 26, 165 (1997).
18. S. Seshadri, G.W. Eldridge, A.K. Agarwal, A.A. Burk and G. Augustine, *Appl. Phys. Lett.* 72, 2026 (1998).
19. T. Troffer, C. Peppermuller, G. Pensl, K. Rottner and A. Schoner, *J. Appl. Phys.* 80, 3739 (1996).
20. M.V. Rao, J. Gardner, P.H. Chi, G. Kelner, J. Kretchmer and M. Ghezzo, *J. Appl. Phys.* 81, 6635 (1997).
21. K. Abe, T. Ohshima, H. Itoh, Y. Aoki, M. Yoshikawa, I. Nashiyama and M. Iwami, *Mater. Sci. Forum* 264-268, 721 (1998).
22. S.K. Ghandhi, *VLSI Fabrication Principles (Silicon and Gallium Arsenide),* (New York: JohnWiley, 1994), Chapters on Diffusion and Ion-Implantation.
23. J.W. Peterson, G. Weyer, H.L. Nielsen, S. Damgaard, W.J. Choyke and H. Andreasen, *Hyperfine Interactions* 23, 17 (1985).
24. W. Wesch, A. Heft, E. Wendler, T. Bachmann and E. Glaser, *Nucl. Instr. Meth. Phys. Res. B.* 96, 335 (1995).
25. O.J. Marsh and H.L. Dunlap, *Rad. Effects* 6, 301 (1970).
26. O.J. Marsh, *Silicon Carbide 1973,* ed. R.C. Marshall, J.W. Faust, Jr. and C.E. Ryan (Columbia, SC: University of South Carolina press 1974), p. 471.
27. L.A. Christel and J.F. Gibbons, *J. Appl. Phys.* 52, 5050 (1981).
28. E. Morvan, J. Monserrat, J. Rebollo, D. Flores, X. Jorda, M.L. Locatelli and L. Ottaviani, *Mater. Sci. Forum* 264, 737 (1998).
29. J.R. Jenny, M. Skowronski, W. C. Mitchel, H.M. Hobgood, R. C. Glass, G. Augustine and R.H. Hopkins, *Silicon Carbide and Related Materials* 1995, 142 (Bristol, U.K.: Institute of Physics, 1996), p. 313.
30. R.C. Glass, G. Augustine, V. Balakrishna, H.M. Hobgood, R.H. Hopkins, J. Jenny, M. Skowronski and W.J. Choyke, *Silicon Carbide and Related Materials 1995,* 142, (Bristol, U.K.: Institute of Physics, 1996), p. 37.
31. J.F. Ziegler, J.P. Biersack and U. Littmark, *The Stopping and Range of Ions in Solids,* (New York: Pergamon, 1985).
32. R.G. Wilson, *Radiat. Effects* 46, 141 (1980).
33. W.K. Hofker, *Philips Res. Rep. Supl.* 8, 41 (1975).
34. S. Ahmed, C.J. Barbero, T.W. Sigmon and J.W. Erickson, *J. Appl. Phys.* 77, 6194 (1995).